

REPRODUCING THE STELLAR MASS/HALO MASS RELATION IN SIMULATED Λ CDM GALAXIES:
THEORY VS OBSERVATIONAL ESTIMATESFERAH MUNSHI^{1,2}, F. GOVERNATO¹, A. M. BROOKS³, C. CHRISTENSEN⁴, S. SHEN⁵, S. LOEBMAN¹, B. MOSTER⁶, T. QUINN¹,
J. WADSLEY⁷,*Draft version February 21, 2022*

ABSTRACT

We examine the present-day total stellar-to-halo mass (SHM) ratio as a function of halo mass for a new sample of simulated field galaxies using fully cosmological, Λ CDM, high resolution SPH + N-Body simulations. These simulations include an explicit treatment of metal line cooling, dust and self-shielding, H_2 based star formation and supernova driven gas outflows. The 18 simulated halos have masses ranging from a few times 10^8 to nearly $10^{12} M_\odot$. At $z=0$ our simulated galaxies have a baryon content and morphology typical of field galaxies. Over a stellar mass range of $2.2 \times 10^3 - 4.5 \times 10^{10} M_\odot$ we find extremely good agreement between the SHM ratio in simulations and the present-day predictions from the statistical Abundance Matching Technique presented in Moster et al. (2012). This improvement over past simulations is due to a number systematic factors, each *decreasing* the SHM ratios: 1) gas outflows that reduce the overall SF efficiency but allow for the formation of a cold gas component 2) estimating the stellar masses of simulated galaxies using artificial observations and photometric techniques similar to those used in observations and 3) accounting for a systematic, up to 30% overestimate in total halo masses in DM-only simulations, due to the neglect of baryon loss over cosmic times. Our analysis suggests that stellar mass estimates based on photometric magnitudes can underestimate the contribution of old stellar populations to the total stellar mass, leading to stellar mass errors of up to 50% for individual galaxies. These results highlight the importance of using proper techniques to compare simulations with observations and reduce the perceived tension between the star formation efficiency in galaxy formation models and in real galaxies.

Subject headings: galaxies: evolution — galaxies: formation — methods: N-Body simulations

1. INTRODUCTION

In the standard Λ Cold Dark Matter (Λ CDM) paradigm (White & Rees 1978; Fall & Efstathiou 1980; Blumenthal et al. 1984; Dekel & Silk 1986; White & Frenk 1991), many galaxy properties are expected to correlate with the mass of the galaxy's host halo. In particular, the stellar-to-halo mass relation (SHM), defined as the ratio of the stellar mass (M_{star}) within a halo of total mass M_{halo} within a given over-density ($\langle \rho \rangle / \rho_{crit} = 200$ in this work) is a robust estimator of the efficiency of gas cooling and star formation (SF) processes over a wide range of halo masses (Somerville & Primack 1999; Bower et al. 2010). Both observational (Heavens et al. 2004; Zheng et al. 2007) and theoretical work (Bower et al. 2011) suggest that the SF efficiency peaks at the scale of L^* galaxies and declines at smaller and larger masses. On the low mass end, this decline is likely because SF is suppressed by gas heating from the UV cosmic field (Quinn et al. 1996; Gnedin 2000; Okamoto et al. 2008;

Nickerson et al. 2011) and supernova (SN) heating with gas removal. At larger masses, energy feedback from super-massive black holes (SMBHs) is thought to be the dominant process responsible for lowering the SF efficiency (Bower et al. 2006; Croton 2009; McCarthy et al. 2011; Johansson et al. 2012).

Recently, Moster et al. (2012, hereafter M12) and other groups (Vale & Ostriker 2004; Conroy et al. 2006; Mandelbaum et al. 2006; More et al. 2009; Guo et al. 2010; Trujillo-Gomez et al. 2011; Behroozi et al. 2012) used the Abundance Matching Technique (AMT) and its variations (Yang et al. 2012) to derive a SHM relation of real galaxies. In its simplest form AMT assumes a monotonic relation between the stellar mass function of (real) galaxies and the underlying halo mass function. This relation is constrained by matching the observed galaxy stellar mass function to the Λ CDM halo mass function from N-body simulations. Similar works (Guo et al. 2010; Leauthaud et al. 2011, 2012) have included constraints from lensing and used slightly different underlying cosmologies. This approach has also been used to constrain the scatter in the SHM (Reddick et al. 2012) by comparing the predicted spatial clustering of DM halos (Sheth et al. 2001; Reed et al. 2007; van Daalen et al. 2012) with the observed abundances and clustering properties of galaxy populations (Blain et al. 2004; Conroy et al. 2006; Reid et al. 2010). Additionally, Behroozi et al. (2012) discuss the implications of the upturn in the faint-end slope of the stellar mass function on the SHM relationship.

Several works have highlighted how uncertainties in the derived SHM relation depend on a number of fac-

¹ Astronomy Department, University of Washington, Box 351580, Seattle, WA, 98195-1580

² e-mail address: fdm@astro.washington.edu

³ Astronomy Department, University of Wisconsin, 475 N. Charter St., Madison, WI, 53706

⁴ Department of Astronomy, University of Arizona, 933 North Cherry Avenue, Rm. N204, Tucson, AZ 85721-0065

⁵ Institute of Particle Physics, University of California, Santa Cruz, CA 95064

⁶ Max-Planck-Institute for Astrophysics, Karl-Schwarzschild-Str. 1, 85741 Garching, Germany

⁷ Department of Physics and Astronomy, McMaster University, Hamilton, ON, Canada L8S 4M1

tors, some of them poorly known. For example the stellar masses of real galaxies are inferred from optical and near-IR photometric measurements and/or resolved spectra (Bell & de Jong 2001; Kauffmann et al. 2003). This approach carries substantial uncertainties and possible degeneracies (Bell & de Jong 2001; Bell et al. 2003; Pforr et al. 2012; Huang et al. 2012; Behroozi et al. 2010) as the observed spectral energy distribution of a galaxy is a function of many physical processes (e.g., stellar evolution, SFH and metal-enrichment history, and wavelength-dependent dust attenuation, Panter et al. 2004). Furthermore, as surveys often measure individual galaxy magnitudes within an aperture based on a surface brightness cutoff, the mass of the stellar component could be systematically underestimated by at least 20% (Graham et al. 2005; Shimasaku et al. 2001) if part of it is old (hence faint) and/or low surface brightness. Finally, the number density of galaxies will be affected by incompleteness at the faint end of the galaxy luminosity function (Dalcanton 1998; Sawala et al. 2011; Geller et al. 2012; Santini et al. 2012). Separate from worries over the stellar mass determinations are worries about the halo mass function. While the halo mass function obtained in DM-only simulations is robustly constrained (Reed et al. 2003; Springel et al. 2005), it has recently (Sawala et al. 2012) been shown that halo masses in DM-only simulations exceed those obtained in simulations including baryon physics by up to 30%, introducing another systematic bias in the AMT, as a galaxy of a given stellar mass is matched with a too massive halo, pushing the stellar-halo mass ratio down. Taken together, the above caveats suggest that a better understanding of the connection between galaxy masses and the underlying halo masses could in principle be gained by using realistic simulations of galaxy formation that directly include baryon physics, SF and SN feedback.

While substantial progress has been made in creating galaxies from cosmological initial conditions (Scannapieco et al. 2010; McCarthy et al. 2012; Sales et al. 2012; Stinson et al. 2012; Johansson et al. 2012), several recent studies have pointed out a large discrepancy between the SHM relation estimated for real galaxies and the one obtained in several numerical simulations of galaxy formation (Sawala et al. 2011; Guo et al. 2010). Simulations have repeatedly shown that a lack of realistic SN feedback leads to overestimating star formation as part of the general overcooling problem (Abadi et al. 2003; Governato et al. 2007; Piontek & Steinmetz 2011; Keres et al. 2011). Most simulations that overproduce stars form galaxies that have large spheroidal components (Eke et al. 2001). Incremental improvements based on more realistic SN feedback (Thacker & Couchman 2000; Stinson et al. 2006) led to simulations that formed galaxies with extended disks (Governato et al. 2009; Brooks et al. 2011), but still substantially overproduced stars. Only recently, a new generation of high resolution simulations demonstrated the impact of feedback at lowering SF efficiency such that SF occurs only at high gas densities (Ceverino & Klypin 2009; Governato et al. 2010; Guedes et al. 2011; Governato et al. 2012; Zolotov et al. 2012; Brook et al. 2012). As SF is more efficient in dense gas clouds, feedback from these high density regions

generate outflows that *simultaneously* improve on several long standing problems namely the substructure overabundance problem (Moore et al. 1998; Klypin et al. 1999; Benson 2010), reducing the B/D ratio in small galaxies by removal of low angular momentum baryons (Binney et al. 2001; Governato et al. 2010; Brook et al. 2011) and forming DM cores by transferring energy from baryons to the DM (Mashchenko et al. 2006; Pasetto et al. 2010; de Souza et al. 2011; Cloet-Osselaer et al. 2012; Macciò et al. 2012; Ogiya & Mori 2012; Pontzen & Governato 2012; Teyssier et al. 2012; Governato et al. 2012). Forming stars in dense gas regions is a crucial step, as observations strongly support that the spatially resolved SF is linked to the local H_2 fraction (Bigiel et al. 2008; Krumholz et al. 2009; Genzel et al. 2012), which only becomes significant at the density of star forming regions, $\geq 10\text{-}100 \text{ amu/cm}^3$.

The relationship between gas density and H_2 abundance can now be naturally implemented in simulations, and the creation and destruction of H_2 can be followed consistently (Gnedin et al. 2009; Christensen et al. 2012), allowing much more realistic simulations to be run, and establishes a physically motivated connection between SF and high density (shielded) gas. This is indeed one of the major steps forward in the work presented here. While feedback from SNe remains still poorly understood, its effects are being observed over a large range of redshifts and galaxy masses (Martin 1999; Wang et al. 2010). It is therefore important to evaluate a new set of high resolution simulations to test if outflows can form galaxies with realistic observational properties that also reside on the SHM relation.

Relatively less attention has been given to comparing results from simulations with observational estimates of the SHM relation in a *consistent* way. While some recent works reported (Sawala et al. 2011; Avila-Reese et al. 2011; Piontek & Steinmetz 2011; Leitner 2012) an excess of stars formed in simulations, they compared the galaxy stellar and total halo masses directly measured from simulations while those quantities are actually inferred from the light distribution of real galaxies. A consistent approach has been already tried with promising results in Oh et al. (2011), where two simulated dwarfs were compared with a set of galaxies from the THINGS survey, finding that the simulations have the same central baryon and DM distribution as in the observational sample. In that work, stellar and halo masses were obtained using photometric and kinematic data for both the simulated and the real sample, finding excellent agreement (see Oh et al. (2011) figure 5).

In this paper, we present a consistent comparison between the SHM estimated in Moster et al. (2012) and a set of high resolution simulations spanning 5 orders of magnitude in stellar masses. The evolution of galaxies is simulated at high resolution using Smoothed Particle Hydrodynamics (SPH) in a cosmological context. We focus on how galaxies populate dark matter halos ranging from $10^8 - 10^{12} M_\odot$ in a field environment and comparing results with the estimates of the SHM from M12. The four most massive, MW-like galaxies have similar resolution to the “Eris” galaxy (Guedes et al. 2011), while the smaller galaxies have even better force resolution (down to 65 pc and star particles as small as $450 M_\odot$).

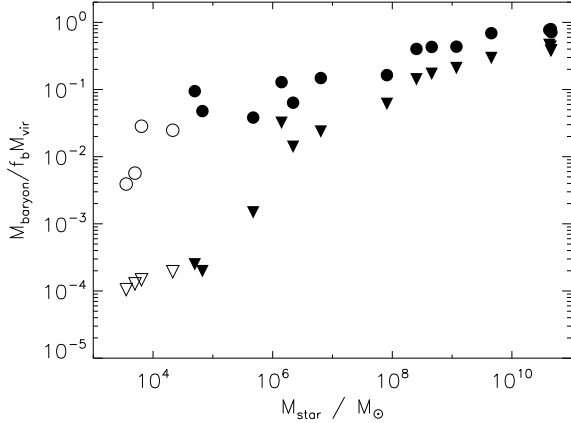


FIG. 1.— *Baryonic fraction with respect to the cosmic ratio, for simulated field galaxies as a function of stellar mass, measured at $z=0$. Circles are the “direct from simulation” results, including all gas and stars within R_{200} . Triangles are the “observable” baryon fractions, including all stars and all the ‘observable’ cold gas (defined as $1.4 \times (\text{HI}+\text{H}_2)$, within R_{200}). The empty symbols are galaxies with no observable gas (cold gas mass $< 100 M_\odot$). Galaxies below $10^8 M_\odot$ lose a significant fraction of baryons due to heating from the cosmic UV background and SN feedback.*

All simulations include the effects of metal line cooling and H_2 dependent star formation.

Our simulations include cooling, star formation, a cosmic UV background and form galaxies with structural properties comparable to the real ones. The dataset utilized is described in detail in Section 2 and has been analyzed in other papers showing that the galaxies follow the Kennicutt-Schmidt law (Christensen et al. 2012), have cored DM profiles similar to the observed ones (Oh et al. 2011; Governato et al. 2012) and realistic satellite populations (Zolotov et al. 2012; Brooks & Zolotov 2012). Without any further fine tuning, in this work we compare the same simulations to the SHM relation obtained in M12, using an analysis technique comparable to the one used in the original paper to estimate their stellar and halo masses. We show that simulations form realistic galactic systems that also match the $z=0$ SHM of real galaxies over five orders of magnitude in stellar mass.

The paper is organized as follows: in §2 we describe the details of our N-body simulations. In §3 we compare results with the SHM predicted in M12. The results are discussed in §4.

2. THE SIMULATIONS

The simulations used in this work were run with the N-Body + SPH code GASOLINE (Wadsley et al. 2004; Stinson et al. 2006) in a fully cosmological ΛCDM context: $\Omega_0 = 0.26$, $\Lambda = 0.74$, $h = 0.73$, $\sigma_8 = 0.77$, $n = 0.96$. The galaxy sample was selected from two uniform DM-only simulations of 25 and 50 Mpc per side. From these volumes a few field-like regions were selected and then resimulated at higher resolution using the ‘zoomed-in’ volume renormalization technique (Katz & White 1993; Pontzen et al. 2008). This technique allows for significantly higher resolution while faithfully capturing the effect of large scale torques that deliver angular momentum to galaxy halos (Barnes & Efstathiou 1987). With this approach, the total high resolution sample contains eighteen field galaxies, each halo resolved by 5×10^4 to a

few 10^6 DM particles within R_{vir} , defined as the radius at which the average halo density $= 200 \times \rho_{\text{crit}}$.

The force spline softening ranges between 64 and 170 pc in the high resolution regions of each volume and it is kept fixed in physical coordinates at $z < 10$. Star particles are formed with a mass of $400\text{--}8000 M_\odot$. The halo mass range covered by the simulations spans nearly four orders of magnitude, from a few times 10^8 to $8 \times 10^{11} M_\odot$ (peak velocities $V_{\text{peak}} = 10$ to 200 km/sec), and stellar masses M_{star} from 10^4 to a few $10^{10} M_\odot$. As other works have highlighted the importance of having a representative sample before drawing general conclusions (Brooks et al. 2011; Sales et al. 2012; McCarthy et al. 2012), the halos in our sample span a representative range of halo spin values and accretion histories (Geha et al. 2006). Galaxies and their parent halos were first identified using AHF⁸ (Gill et al. 2004; Knollmann & Knebe 2009). The total halo mass (including DM, gas and stars) is defined at a radius R_{vir} , defined as the radius at which the average halo density $= 200 \times \rho_{\text{crit}}$, consistent with M12. No sub-halos have been included in our sample, although the most massive galaxies have a realistic population of satellites (Zolotov et al. 2012). More details on this dataset and the properties of the satellite population are given in Governato et al. (2012) and Brooks & Zolotov (2012).

2.1. H_2 fraction, Star Formation and SN Feedback

In a significant improvement, this new set of simulations include metal line cooling (Shen et al. 2010) and a dust dependent description of H_2 creation and destruction by Lyman-Werner radiation and shielding of HI and H_2 (Gnedin et al. 2009; Christensen et al. 2012, hereafter CH12). As in CH12, the star formation rate (SFR) in our simulations is set by the local gas density and the H_2 fraction; $\text{SF} \propto (f_{\text{H}_2} \times \rho_{\text{gas}})^{1.5}$. A SF effi-

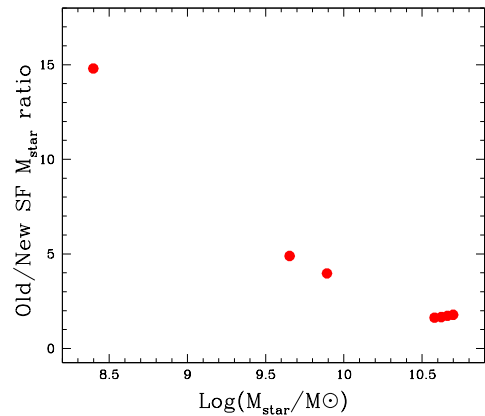


FIG. 2.— *The stellar mass ratio between the galaxies simulated with the old ‘low density SF threshold’ and the new sample. In the new sample SF is regulated by the local abundance of molecular hydrogen, resulting in feedback significantly lowering the total SF efficiency. All quantities as measured directly from the simulations.*

⁸ AMIGA’s Halo Finder, available for download at <http://popia.ft.uam.es/AHF/Download.html>

ciency parameter, $c_* = 0.1$, gives the correct normalization of the Kennicutt-Schmidt relation (the SF efficiency for each star forming region is much lower than the implied 10%, as only a few star particles are formed before gas is disrupted by SN winds). With the inclusion of the H_2 fraction term (see also Kuhlen et al. 2011), the efficiency of SF drops to zero in warm gas with $T > 3,000$ K. The simulations include a scheme for turbulent mixing that redistributes heavy elements among gas particles (Shen et al. 2010). With this approach, the *local* SF efficiency is linked to the local H_2 abundance, as regulated by the gas metallicity and the radiation field from young stars, without having to resort to simplified approaches based on a fixed local gas density threshold (Governato et al. 2010; Kuhlen et al. 2011). The simulations assumed a Kroupa IMF and relative yields, but observable quantities have been converted to a Chabrier IMF, for a direct comparison with Moster et al. (2012).

As in previous works using the “blastwave” SN feedback approach (Stinson et al. 2006; Governato et al. 2012), mass, thermal energy, and metals are deposited into nearby gas when massive stars evolve into SNe. The amount of energy deposited amongst those neighbors is 10^{51} ergs per SN event. Gas cooling is then turned off until the end of the momentum-conserving phase of the SN blastwave which is set by the local gas density and temperature and by the total amount of energy injected, typically a few million years. Equilibrium rates are computed from the photoionization code Cloudy (Ferland et al. 1998), following Shen et al. (2010). A spatially uniform, time evolving, cosmic UV background turns on at $z = 9$ and modifies the ionization and excitation state of the gas, following an updated model of Haardt & Madau (1996).

This feedback model differs compared to other “sub-grid” schemes (e.g., Springel & Hernquist 2003; Scannapieco et al. 2012) in that it keeps gas hydrodynamically coupled while in galactic outflows. The ef-

ficient deposition of SN energy into the ISM, and the modeling of recurring SN by the Sedov solution, should be interpreted as a scheme to model the effect of energy deposited in the local ISM by *all* processes related to young stars, including UV radiation from massive stars (Hopkins et al. 2011; Wise et al. 2012). The SFHs of the galaxies in our simulated sample are bursty, especially those residing in halos smaller than $10^{10} M_\odot$. As discussed in Brook et al. (2011) and Pontzen & Governato (2012), a bursty SFH is necessary to remove low angular momentum baryons and create the fast outflows able to transfer energy from baryons to the DM component and create DM cores (Governato et al. 2010). These processes lead to realistic dwarf galaxies with slowly rising rotation curves and typical central surface brightnesses $21 < \mu_{B,o} < 23.5$ (Oh et al. 2011). Outflows and the cosmic UV field progressively suppress star formation in halos with total mass smaller than a few $10^{10} M_\odot$. Test runs verify that the effect of energy feedback on suppressing SF is much larger than that of having a low H_2 fraction-SF efficiency (Christensen et al. 2012).

2.2. Star formation efficiency as a function of galaxy halo mass

As a result of SF feedback processes, the SF efficiency is greatly reduced over the whole mass range of our simulated sample. The smallest galaxies in our sample turn only $\sim 0.01\%$ of their primordial baryons into stars. The more massive galaxies in our sample turn $\sim 30\%$ of their primordial baryon content into stars, but we demonstrate in the next section that using stellar masses based on photometry reduces this efficiency to an apparent 10%. Feedback expels about 70% of the gas to outside of R_{vir} in dwarf galaxies with $v_c \sim 40\text{--}50 \text{ km s}^{-1}$. Larger galaxies retain a larger fraction of their original baryons, while the smallest galaxies lose an even larger fraction of baryons due to gas heating by the cosmic UV background, which further reduces their SF (see Figure 1).

To evaluate the effect of the adopted SF model on the resulting SF efficiency of our galaxy sample, galaxies were re-simulated using the SF approach used in our older works. These reference runs adopt a lower density threshold for SF, 0.1 amu/cm^3 . As discussed in several works (Governato et al. 2010; Guedes et al. 2011), a low density threshold makes SF more diffuse and locally less efficient. In this scenario, typical of low resolution simulations where star forming regions cannot be resolved, the amount of SN energy per unit mass delivered to gas particles is effectively lowered, making feedback much less effective at suppressing SF. While the galaxies in the low threshold sample have realistic disk sizes (Brooks et al. 2011) and the total amount of energy released into the gas is actually a few times larger, they contain many times more stars (see Figure 2) and overproduce stars compared to the SHM relation. The comparison between the amount of stars formed in the old and the new runs (Figure 2) demonstrates that the large decrease in the SF efficiency in the new simulations (as much as a factor of 15) is due to the improved implementation of SF in dense/ H_2 rich regions (see also Governato et al. 2010). This lower SF efficiency goes a long way toward reconciling simulations of galaxy formation with current estimates of the SHM relation.

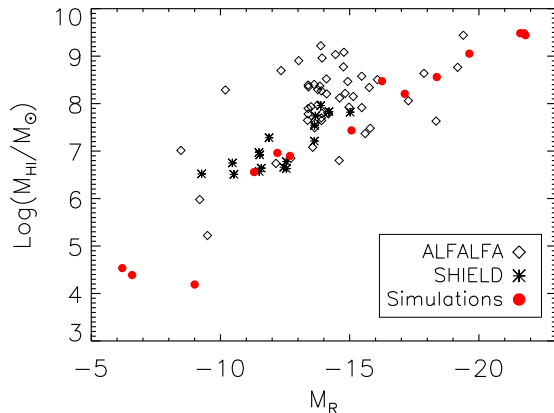


FIG. 3.— *The cold gas mass as a function of stellar mass. Simulations vs. SHIELD and ALFALFA data.* The HI mass of each galaxy in the simulated sample is plotted vs the SDSS r -band magnitude and compared to two samples from nearby surveys. Red solid dots: simulations. Diamonds: ALFALFA survey. Asterisks: SHIELD survey. While feedback removes a large fraction of the primordial baryons, the simulated galaxies have a high gas/stellar mass ratio, comparable to the observed samples. Most of the cold gas resides within a few disk scale lengths from the simulated galaxy centers.

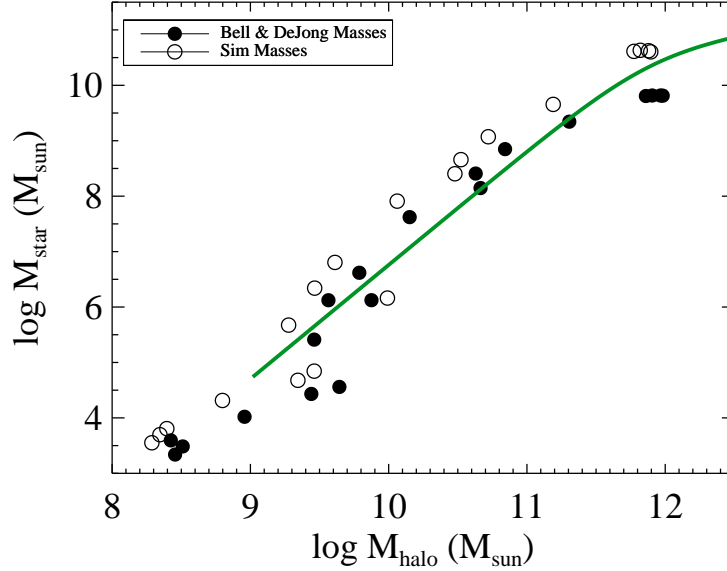


FIG. 4.— *The Stellar Mass vs Halo Mass*. Black Solid Dots: The SHM relation from our simulations set with stellar masses measured using Petrosian magnitudes and halo masses from DM-only runs. This procedure mimics the one followed in M12. Open Dots: Unbiased stellar masses measured directly from the simulations. Solid Line: Observational results from M12.

2.3. The Baryon Content of the Simulated Galaxies

The more massive galaxies in our sample are disk dominated, transitioning to irregular galaxies below $\sim 10^{10} M_{\odot}$. The outflows (and the UV cosmic field in halos below $\sim 10^9 M_{\odot}$) significantly lower the baryon fraction of the host halos, with a strong trend of lower baryon fractions at smaller halo (stellar) mass (see Figure 1). However, because the fraction of remaining gas turned into stars is low at all galaxy masses and especially in dwarfs, the galaxies in our sample have relatively high cold gas to stellar mass ratios, typical of real galaxies over the tested range. In Figure 3 we compare the cold gas (HI) content of the simulated sample to the nearby HI surveys ALFALFA (Giovanelli et al. 2005) and SHIELD (Cannon et al. 2011). The observed dataset includes only galaxies closer than the Virgo cluster, for a better comparison with our sample of field galaxies. With the caveat that selection effects can still play a role, there is very good agreement between simulations and observations.

The HI masses are directly measured from the simulations, where HI and H_2 ⁹ abundances are calculated on the fly. Magnitudes are measured in the SDSS *r*-band.

We verified that the cold gas fraction in the comparison runs adopting a low density threshold for SF is about a factor of ten lower at all halo masses. Lower resolution simulations of small mass systems have often reported the formation of relatively gas poor galaxies (Governato et al. 2007; Colín et al. 2010; Avila-Reese et al. 2011; Sawala et al. 2011). Low gas content in simulated low-*z* galaxies is likely due to a high efficiency of gas to stars conversion (Piontek & Steinmetz 2011) and/or to an excessive loading factor of the SN winds.

⁹ note that H_2 masses are small and, while neglected in Figure 3, contribute little to the overall cold gas mass

3. THE STELLAR MASS - HALO MASS RELATION

Once individual galaxies in our sample have been identified with AHF, the Stellar Mass - Halo Mass ratio for each galaxy can then be obtained. The definition of “halo mass” includes all DM and baryons within an overdensity of 200, but not the mass associated with individual satellites (a few % of total at the most). All stars not in satellites, but within R_{200} are associated with the central galaxy in the halo. This simple approach is similar to what has been done in several previous works (Sawala et al. 2011; Brook et al. 2012) and similar to what has been used in previous comparisons between simulations and the SHM relation obtained using the AMT (Guo et al. 2010; Moster et al. 2012). Our new sample of simulated field galaxies (open circles in Figure 4) follows closely the shape and normalization of the present day SHM relation presented in M12 over the 10^9 – $10^{12} M_{\odot}$ halo mass range (solid line), with $M_{\text{star}} \propto M_{\text{halo}}^2$. This is a large improvement over most published works and confirms results on smaller samples (Governato et al. 2010; Oh et al. 2011; Guedes et al. 2011; Brook et al. 2012) that adopted similar SF and feedback recipes.

Clearly, an approach where a) SF is limited to dense, H_2 -rich gas clouds (a highly correlated situation, see Christensen et al. 2012) and b) feedback is hydrodynamically coupled to outflows significantly reduces the SF efficiency and the present day stellar mass in galaxy sized halos over a wide mass range. Our simulations show that both a) and b) are alone not sufficient, but the combination is sufficient. We have first verified that in the absence of feedback the SF efficiency remains high even if the consumption rate of gas is long, as over the course of a Hubble time most cold gas within the galaxy eventually turns into stars. Moreover, lack of SN feedback fails to remove the low angular momentum gas, originating galaxies with an excessive spheroidal component

(Governato et al. 2010; Brook et al. 2011). Similarly, if the identical SN feedback recipe used in this work is applied to simulations where SF is allowed in cold, but relatively low density gas (e.g 0.1 amu, as often adopted in the past), it fails to significantly lower the overall SF efficiency. In our sample, the mass in stars formed by $z = 0$ in galaxies with H_2 /high density regulated SF is lower by as much as fifteen compared to simulations of the same halos adopting a lower density threshold. The overproduction of stars in the low threshold runs occurs *even* when metal lines cooling is neglected.

In summary, while the SF efficiency in the high threshold simulations is lower, the cold gas content is similar to that observed in real galaxies (see §2.3). Hence, a low SF efficiency was not obtained by simply increasing the feedback strength and “blowing away” all the baryons. Combined, these results show that adopting a more realistic description of *where* stars form and how feedback regulates SF leads to realistic simulations of galaxies.

However, for a meaningful comparison with observations and the SHM inferred in M12, it is important to infer *both* the stellar and halo mass from the simulations using the same techniques as the observations. This additional step is necessary as simulations directly measure the *mass distribution*, while observations infer the stellar mass from the *light distribution*. Below we show that this more accurate approach affects the results substantially. We will provide, for the first time, an accurate comparison with the present day SHM relation obtained from observational data. We used the following procedure:

- Magnitudes based on the age and metallicity of each star particle were derived using the Starburst99 stellar population synthesis models of Leitherer et al. (1999) and Vázquez & Leitherer (2005), adopting a Kroupa (2001) IMF.
- For each simulated galaxy, Petrosian aperture magnitudes (Blanton et al. 2001; Yasuda et al. 2001) were obtained in the r band. This step is necessary as observations are limited by the surface brightness of the target galaxy dropping below the sky brightness. This systematic bias underestimates the amount of light associated with individual galaxies, and it is estimated to be of the order of 20% for real galaxies (Dalcanton 1998; Blanton et al. 2001). As our galaxies have light profiles that closely mimic those of real galaxies (Brooks et al. 2011), applying this constraint is appropriate. We verified that the amount of light lost is similar to that estimated for observational samples.
- The stellar mass of each galaxy was then estimated based on its B-V color and V total magnitude, assuming a Salpeter IMF to be consistent with adopting the same fitting formula as in Bell & de Jong (2001), namely $L_V = 10^{-(V-4.8)/2.5}$ and then $M_{star} = L_V \times 10^{-0.734+1.404 \times (B-V)}$. We then utilize a conversion from Salpeter to Chabrier IMF to remain consistent with M12. We find that this procedure systematically *underestimates* the true stellar masses (by summing all star particles within R_{vir} not in satellites) of galaxies by 20-30%.

This result extends over the whole range of galaxy masses. We find that the specific criteria adopted in Bell & de Jong (2001) tends to underestimate the contribution from old (i.e., high M/L) stellar populations.

- The halo mass for each simulated galaxy was measured re-running each simulation as DM-only, matching halos between the two runs and counting all mass with R_{vir} (again defined as the radius within which the average overdensity is $< \rho > = 200\rho_{crit}$). This step is necessary to follow the procedure adopted in Moster et al. (2012), where halo masses were obtained from a large cosmological simulation that did not include gas physics. This procedure avoids a subtle, but significant and systematic bias between the total halo mass measured in DM-only runs vs those of the same halos in simulations that include gas physics and feedback. In the latter simulations, feedback can remove a significant fraction of the baryons from the halo, decreasing the total mass within a fixed physical radius. The virial radius, if defined at a fixed overdensity, then shrinks, leading to a smaller total halo mass. The decrease in M_{vir} varies with mass, as it depends on the amount of baryons lost, but it can be significant, up to 30%. Since the lowest mass galaxies in our sample have lost the most baryons (in winds and UV background heating), they can experience a decrease of $\sim 30\%$ in halo mass. At the high mass end, where galaxies retain most of their baryons, the simulated galaxies still see a change of 5-10% in total halo mass compared to the DM-only run (where obviously no baryon mass loss is possible). These results are consistent with estimates in (Sawala et al. 2012). Sawala et al. (2012) also interprets this shift as a systematic reduction in the matter infall rate. As even small amounts of baryons are removed, the gravitational attraction on surrounding material decreases, leading to a decrease in the infall rate of both gas and DM and, overtime, to a smaller halo mass. Neglecting this effect results in moving the simulations datapoints *to the left*, away from the SHM relation inferred using DM-only runs. This bias is particularly noticeable at small galaxy masses, where the SHM relation is steeper.

In Figure 4, the black solid dots show results from our simulations dataset, but using the procedure outlined above, which closely matches that adopted in M12. The normalization of the SHM is $\sim 40\%$ lower than that inferred using the simulations quantities at face value and closer overall to the SHM relation of M12. There is very good agreement between the SHM inferred from the ‘artificial observations’ and the fit in M12 over at least 4 orders of magnitude in halo mass. The mass of the brightest galaxies (close in mass and morphology to Milky Way analogues) goes from being higher to being slightly *lower* than the SHM. This result confirms that the “blastwave” feedback implementation is able to reduce the SF efficiency not only at small halo masses but also in present day halos around $10^{12} M_\odot$ (see also Guedes et al. 2011).

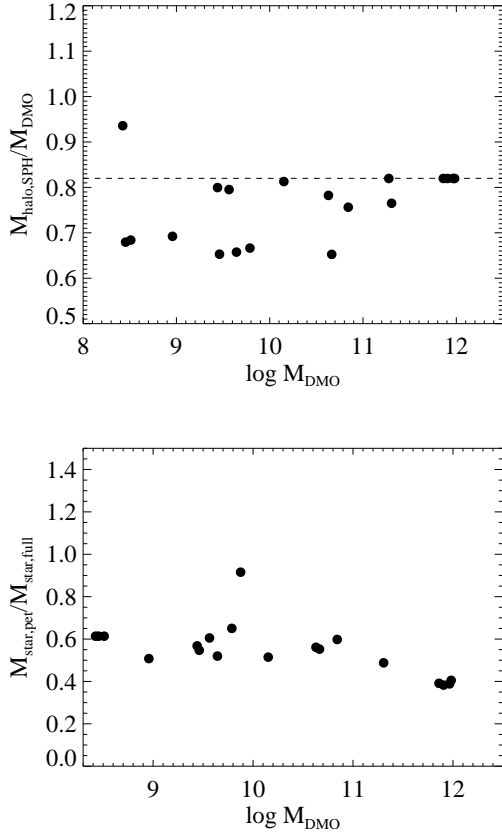


FIG. 5.— Top Panel: *Halo mass ratio of galaxies in runs with baryons and SF vs DM-only runs.* Individual halos in DM-only runs are typically 30% more massive than their counterparts in simulations with gas physics and SF. The effect is smaller in more massive halos, where baryon loss due to feedback is less (see also Sawala et al. (2012)). The dashed horizontal line marks the ratio if halos had a 100% baryon loss. Bottom panel: *Estimated vs. True Stellar Mass as a function of halo mass.* The stellar mass using artificial Petrosian magnitudes and measured using the photometric method in (Bell & de Jong 2001) vs the “true” Stellar mass measured directly from the simulations. Stellar masses measured using the photometric method in (Bell & de Jong 2001) in combination with the flux loss from applying the petrosian magnitudes are underestimated by about 50% across the range of galaxy masses in our study.

In Figure 5a we show the total halo mass ratio between the simulations that include baryons and SF vs the DM-only ones. As discussed above, halos in DM-only runs are consistently (and significantly, about 30%) more massive. In Figure 5b we show the ratio between the stellar masses obtained using a combination of Petrosian Magnitudes with Bell & de Jong (2001) M/L ratios (closely following M12) and stellar masses derived directly from the simulations. A systematic bias of about 50% is evident across the whole mass range. The results from this section highlight the importance of a careful comparison between simulations and observations. This approach further reinforces our findings that the modeling of SN feedback greatly reduces the tension between the present time SHM relation inferred from the Abundance Matching Technique for halos with total mass $< 10^{12} M_{\odot}$ and the predictions from hydrodynamical simulations in a cosmological context. Without fine tuning, this better agreement also preserves the morphology of

the galaxies formed, with disk-dominated massive galaxies and low mass irregulars that are gas rich. In future work, we plan to extend this approach to higher redshifts, using the appropriate criteria to measure stellar masses in high- z galaxies (e.g., Pforr et al. 2012; Maraston et al. 2012).

4. CONCLUSIONS

We have measured the SHM (stellar mass – halo mass) relation for a set of field galaxies simulated in a Λ CDM cosmology and compared it with the redshift zero predictions based on data from the SDSS and the Abundance Matching Technique described in M12. The comparison revealed very good agreement in normalization and shape over five orders of magnitude in stellar mass. The new simulations include an explicit description of metal lines cooling and H_2 regulated SF, and SN driven outflows. The combination of SF driven by the local efficiency of H_2 and outflows reduce the overall SF efficiency over the whole Hubble time by almost an order of magnitude compared to older simulations, with resulting $M_{\text{star}} \propto M_{\text{halo}}^2$. While a large fraction of baryons is expelled, especially in halos smaller than $10^{11} M_{\odot}$, the resulting galaxies have an HI content comparable to those inferred by local surveys, namely ALFALFA and SHIELD. The same galaxy set has a cored central DM density distribution, similar to observations of real galaxies (Governato et al. 2012; Brooks & Zolotov 2012).

This agreement between simulations and observational data is due to two systematic factors: 1) An implementation of SF that relates the SF efficiency to the local H_2 abundance in resolved star forming regions, resulting in localized feedback that significantly lowers the SF efficiency and 2) “observing” the simulations to properly compare them to observational estimates of the SHM relation. This approach involved creating artificial photometric light profiles of the simulated galaxies and estimating stellar masses based on aperture magnitudes. Importantly, it also requires coupling the stellar masses to halo masses derived from DM-only simulations, rather than the baryonic simulations. Our analysis shows that adopting photometric stellar masses contributes to a 20-30% *systematic* reduction in the estimated stellar masses. Stellar mass estimates based on one band photometric magnitudes are likely to underestimate the contribution of old stellar populations (reflecting the larger contribution to the total flux coming from younger stars). This systematic effect is further exacerbated by the use of aperture based magnitudes, adding another 20-30% due to neglecting the contribution of low surface brightness populations. Finally, a third systematic effect comes from a difference in halo masses in collisionless (DM-only) simulations vs simulations including baryon physics and outflows. Baryon mass loss makes halo masses smaller by up to 30% when calculated at the same overdensity (200 in our paper and M12). The effect of removing these biases is to move the simulation points in Figure 4 further lower and to the right, closer to the SHM.

Notwithstanding the improvements described in this and other recent works, further adjustment to our numerical schemes to model SF and feedback processes are most likely required, as more observational constraints become available and our understanding of SF improves.

In future work we plan to extend our analysis of the stellar mass – halo mass relation to higher redshifts and larger galaxy masses. The results presented in M12 point to a possible discrepancy between the shape of the star formation history of real galaxies vs the simulated ones. Given the difficulty to obtain robust estimates from faint and distant galaxy samples, we expect that the approach outlined in this work, i.e. creating artificial observations to more directly compare simulations with observations, will play an important role.

ACKNOWLEDGMENTS

FM, FG and TQ were funded by NSF grant AST-0908499. FG acknowledges support from NSF grant AST-0607819 and NASA ATP NNX08AG84G. AB acknowledges support from The Grainger Foundation. Simulations were run at TACC and NAS. We thank Oleg Gnedin, Piero Madau, Javiera Guedes for useful discussions. We thank Jessica Rosenberg for ALFALFA data.

REFERENCES

- Abadi, M. G., Navarro, J. F., Steinmetz, M., & Eke, V. R. 2003, *ApJ*, 591, 499
- Avila-Reese, V., Colín, P., González-Samaniego, A., Valenzuela, O., Firmani, C., Velázquez, H., & Ceverino, D. 2011, *ApJ*, 736, 134
- Barnes, J., & Efstathiou, G. 1987, *ApJ*, 319, 575
- Behroozi, P. S., Conroy, C., & Wechsler, R. H. 2010, *ApJ*, 717, 379
- Behroozi, P. S., Wechsler, R. H., & Conroy, C. 2012, *ArXiv e-prints*
- Bell, E. F., & de Jong, R. S. 2001, *ApJ*, 550, 212
- Bell, E. F., McIntosh, D. H., Katz, N., & Weinberg, M. D. 2003, *ApJS*, 149, 289
- Benson, A. J. 2010, 495, 33
- Bigiel, F., Leroy, A., Walter, F., Brinks, E., de Blok, W. J. G., Madore, B., & Thornley, M. D. 2008, *AJ*, 136, 2846
- Binney, J., Gerhard, O., & Silk, J. 2001, *MNRAS*, 321, 471
- Blain, A. W., Chapman, S. C., Smail, I., & Ivison, R. 2004, *ApJ*, 611, 725
- Blanton, M. R., et al. 2001, *AJ*, 121, 2358
- Blumenthal, G. R., Faber, S. M., Primack, J. R., & Rees, M. J. 1984, *Nature*, 311, 517
- Bower, R. G., Benson, A. J., & Crain, R. A. 2011, *ArXiv e-prints*
- Bower, R. G., Benson, A. J., Malbon, R., Helly, J. C., Frenk, C. S., Baugh, C. M., Cole, S., & Lacey, C. G. 2006, *MNRAS*, 370, 645
- Bower, R. G., Vernon, I., Goldstein, M., Benson, A. J., Lacey, C. G., Baugh, C. M., Cole, S., & Frenk, C. S. 2010, *MNRAS*, 407, 2017
- Brook, C. B., Stinson, G., Gibson, B. K., Wadsley, J., & Quinn, T. 2012, *MNRAS*, 424, 1275
- Brook, C. B., et al. 2011, *MNRAS*, 415, 1051
- Brooks, A. M., & Zolotov, A. 2012, *ArXiv e-prints*
- Brooks, A. M., et al. 2011, *ApJ*, 728, 51
- Cannon, J. M., et al. 2011, *ApJ*, 739, L22
- Ceverino, D., & Klypin, A. 2009, *ApJ*, 695, 292
- Christensen, C., Quinn, T., Governato, F., Stilp, A., Shen, S., & Wadsley, J. 2012, *ArXiv e-prints*
- Cloet-Osselaer, A., De Rijcke, S., Schroyen, J., & Dury, V. 2012, *MNRAS*, 2952
- Colín, P., Avila-Reese, V., Vázquez-Semadeni, E., Valenzuela, O., & Ceverino, D. 2010, *ApJ*, 713, 535
- Conroy, C., Wechsler, R. H., & Kravtsov, A. V. 2006, *ApJ*, 647, 201
- Croton, D. J. 2009, *MNRAS*, 394, 1109
- Dalcanton, J. J. 1998, *ApJ*, 495, 251
- de Souza, R. S., Rodrigues, L. F. S., Ishida, E. E. O., & Opher, R. 2011, *MNRAS*, 415, 2969
- Dekel, A., & Silk, J. 1986, *ApJ*, 303, 39
- Eke, V. R., Navarro, J. F., & Steinmetz, M. 2001, *ApJ*, 554, 114
- Fall, S. M., & Efstathiou, G. 1980, *MNRAS*, 193, 189
- Ferland, G. J., Korista, K. T., Verner, D. A., Ferguson, J. W., Kingdon, J. B., & Verner, E. M. 1998, *PASP*, 110, 761
- Geha, M., Blanton, M. R., Masjedi, M., & West, A. A. 2006, *ApJ*, 653, 240
- Geller, M. J., Diaferio, A., Kurtz, M. J., Dell’Antonio, I. P., & Fabricant, D. G. 2012, *AJ*, 143, 102
- Genzel, R., et al. 2012, *ApJ*, 746, 69
- Gill, S. P. D., Knebe, A., & Gibson, B. K. 2004, *MNRAS*, 351, 399
- Giovanelli, R., et al. 2005, *AJ*, 130, 2598
- Gnedin, N. Y. 2000, *ApJ*, 542, 535
- Gnedin, N. Y., Tassis, K., & Kravtsov, A. V. 2009, *ApJ*, 697, 55
- Governato, F., Willman, B., Mayer, L., Brooks, A., Stinson, G., Valenzuela, O., Wadsley, J., & Quinn, T. 2007, *MNRAS*, 374, 1479
- Governato, F., et al. 2009, *MNRAS*, 398, 312
- . 2010, *Nature*, 463, 203
- . 2012, *MNRAS*, 422, 1231
- Graham, A. W., Driver, S. P., Petrosian, V., Conselice, C. J., Bershady, M. A., Crawford, S. M., & Goto, T. 2005, *AJ*, 130, 1535
- Guedes, J., Callegari, S., Madau, P., & Mayer, L. 2011, *ApJ*, 742, 76
- Guo, Q., White, S., Li, C., & Boylan-Kolchin, M. 2010, *MNRAS*, 404, 1111
- Haardt, F., & Madau, P. 1996, *ApJ*, 461, 20
- Heavens, A., Panter, B., Jimenez, R., & Dunlop, J. 2004, *Nature*, 428, 625
- Hopkins, P. F., Quataert, E., & Murray, N. 2011, *ArXiv e-prints*
- Huang, S., Haynes, M. P., Giovanelli, R., Brinchmann, J., Stierwalt, S., & Neff, S. G. 2012, *ArXiv e-prints*
- Johansson, P. H., Naab, T., & Ostriker, J. P. 2012, *ArXiv e-prints*
- Katz, N., & White, S. D. M. 1993, *ApJ*, 412, 455
- Kauffmann, G., et al. 2003, *MNRAS*, 341, 33
- Keres, D., Vogelsberger, M., Sijacki, D., Springel, V., & Hernquist, L. 2011, *ArXiv e-prints*
- Klypin, A., Kravtsov, A. V., Valenzuela, O., & Prada, F. 1999, *ApJ*, 522, 82
- Knollmann, S. R., & Knebe, A. 2009, *ApJS*, 182, 608
- Krumholz, M. R., McKee, C. F., & Tumlinson, J. 2009, *ApJ*, 699, 850
- Kuhlen, M., Krumholz, M., Madau, P., Smith, B., & Wise, J. 2011, *ArXiv e-prints*
- Leauthaud, A., et al. 2011, *ArXiv e-prints*
- . 2012, *ApJ*, 744, 159
- Leitner, C., et al. 1999, *ApJS*, 123, 3
- Leitner, S. N. 2012, *ApJ*, 745, 149
- Maccio, A. V., Stinson, G., Brook, C. B., Wadsley, J., Couchman, H. M. P., Shen, S., Gibson, B. K., & Quinn, T. 2012, *ApJ*, 744, L9
- Mandelbaum, R., Seljak, U., Kauffmann, G., Hirata, C. M., & Brinkmann, J. 2006, *MNRAS*, 368, 715
- Maraston, C., et al. 2012, *ArXiv e-prints*
- Martin, C. L. 1999, *ApJ*, 513, 156
- Mashchenko, S., Couchman, H. M. P., & Wadsley, J. 2006, *Nature*, 442, 539
- McCarthy, I. G., Schaye, J., Bower, R. G., Ponman, T. J., Booth, C. M., Dalla Vecchia, C., & Springel, V. 2011, *MNRAS*, 412, 1965
- McCarthy, I. G., Schaye, J., Font, A. S., Theuns, T., Frenk, C. S., Crain, R. A., & Dalla Vecchia, C. 2012, *ArXiv e-prints*
- Moore, B., Governato, F., Quinn, T., Stadel, J., & Lake, G. 1998, *ApJ*, 499, L5+
- More, S., van den Bosch, F. C., & Cacciato, M. 2009, *MNRAS*, 392, 917
- Moster, B. P., Naab, T., & White, S. D. M. 2012, *ArXiv e-prints*
- Nickerson, S., Stinson, G., Couchman, H. M. P., Bailin, J., & Wadsley, J. 2011, *MNRAS*, 415, 257
- Ogiya, G., & Mori, M. 2012, *ArXiv e-prints*
- Oh, S.-H., Brook, C., Governato, F., Brinks, E., Mayer, L., de Blok, W. J. G., Brooks, A., & Walter, F. 2011, *AJ*, 142, 24
- Okamoto, T., Gao, L., & Theuns, T. 2008, *MNRAS*, 390, 920
- Panther, B., Heavens, A. F., & Jimenez, R. 2004, *MNRAS*, 355, 764

- Pasetto, S., Grebel, E. K., Berczik, P., Spurzem, R., & Dehnen, W. 2010, *A&A*, 514, A47
- Pforr, J., Maraston, C., & Tonini, C. 2012, ArXiv e-prints
- Piontek, F., & Steinmetz, M. 2011, *MNRAS*, 410, 2625
- Pontzen, A., & Governato, F. 2012, *MNRAS*, 421, 3464
- Pontzen, A., et al. 2008, *MNRAS*, 390, 1349
- Quinn, T., Katz, N., & Efstathiou, G. 1996, *MNRAS*, 278, L49
- Reddick, R. M., Wechsler, R. H., Tinker, J. L., & Behroozi, P. S. 2012, ArXiv e-prints
- Reed, D., Gardner, J., Quinn, T., Stadel, J., Fardal, M., Lake, G., & Governato, F. 2003, *MNRAS*, 346, 565
- Reed, D. S., Governato, F., Quinn, T., Stadel, J., & Lake, G. 2007, *MNRAS*, 378, 777
- Reid, B. A., et al. 2010, *MNRAS*, 404, 60
- Sales, L. V., Navarro, J. F., Theuns, T., Schaye, J., White, S. D. M., Frenk, C. S., Crain, R. A., & Dalla Vecchia, C. 2012, *MNRAS*, 3041
- Santini, P., et al. 2012, *A&A*, 538, A33
- Sawala, T., Frenk, C. S., Crain, R. A., Jenkins, A., Schaye, J., Theuns, T., & Zavala, J. 2012, ArXiv e-prints
- Sawala, T., Guo, Q., Scannapieco, C., Jenkins, A., & White, S. 2011, *MNRAS*, 413, 659
- Scannapieco, C., Gadotti, D. A., Jonsson, P., & White, S. D. M. 2010, *MNRAS*, 407, L41
- Scannapieco, C., et al. 2012, *MNRAS*, 423, 1726
- Shen, S., Wadsley, J., & Stinson, G. 2010, *MNRAS*, 407, 1581
- Sheth, R. K., Mo, H. J., & Tormen, G. 2001, *MNRAS*, 323, 1
- Shimasaku, K., et al. 2001, *AJ*, 122, 1238
- Somerville, R. S., & Primack, J. R. 1999, *MNRAS*, 310, 1087
- Springel, V., & Hernquist, L. 2003, *MNRAS*, 339, 312
- Springel, V., et al. 2005, *Nature*, 435, 629
- Stinson, G., Brook, C., Macciò, A. V., Wadsley, J., Quinn, T. R., & Couchman, H. M. P. 2012, ArXiv e-prints
- Stinson, G., Seth, A., Katz, N., Wadsley, J., Governato, F., & Quinn, T. 2006, *MNRAS*, 373, 1074
- Teyssier, R., Pontzen, A., Dubois, Y., & Read, J. 2012, ArXiv e-prints
- Thacker, R. J., & Couchman, H. M. P. 2000, *ApJ*, 545, 728
- Trujillo-Gomez, S., Klypin, A., Primack, J., & Romanowsky, A. J. 2011, *ApJ*, 742, 16
- Vale, A., & Ostriker, J. P. 2004, *MNRAS*, 353, 189
- van Daalen, M. P., Angulo, R. E., & White, S. D. M. 2012, ArXiv e-prints
- Vázquez, G. A., & Leitherer, C. 2005, *ApJ*, 621, 695
- Wadsley, J. W., Stadel, J., & Quinn, T. 2004, *New Astronomy*, 9, 137
- Wang, P., Li, Z., Abel, T., & Nakamura, F. 2010, *ApJ*, 709, 27
- White, S. D. M., & Frenk, C. S. 1991, *ApJ*, 379, 52
- White, S. D. M., & Rees, M. J. 1978, *MNRAS*, 183, 341
- Wise, J. H., Abel, T., Turk, M. J., Norman, M. L., & Smith, B. D. 2012, ArXiv e-prints
- Yang, X., Mo, H. J., van den Bosch, F. C., Zhang, Y., & Han, J. 2012, *ApJ*, 752, 41
- Yasuda, N., et al. 2001, *AJ*, 122, 1104
- Zheng, Z., Coil, A. L., & Zehavi, I. 2007, *ApJ*, 667, 760
- Zolotov, A., et al. 2012, ArXiv e-prints